

Journal of Nanotechnology & Advanced Materials

An International Journal

@ 2014 NSPNatural Sciences Publishing Cor.

http://dx.doi.org/10.12785/jnam/020102

Vibrational Spectroscopic [IR and Raman] Analysis and Computational Investigation [NMR, UV-Visible, MEP and Kubo gap] on L-Valinium Picrate

I. John David Ebenezar¹, S. Ramalingam^{2,*}, C. Ramachandra Raja³ and P. C. Jobe Prabakar¹

¹ Department of Physics, TBML College, Porayar, Tamil Nadu, India

² Department of Physics, A.V.C. College, Mayiladuthurai, Tamilnadu, India

³ Department of Physics, Government Arts College, Kumbakonam, Tamilnadu, India

*Email: ramalingam.physics@gmail.com

Received: 16 May 2013; Revised: 9 June 2013; Accepted: 28 June 2013

Abstract: In the present methodical study, FT-IR, FT-Raman and NMR spectra of the L-Valinium Picrate are recorded and the fundamental vibrational frequencies are tabulated and assigned. The Gaussian hybrid computational calculations are carried out by HF and DFT (LSDA, B3LYP and B3PW91) methods with 6-311++G(d,p) basis sets and the corresponding results are compared with experimental values. The existence of vanderwals interaction between L-Valine and picric acid is investigated. The Zwitterionic motion of hydrogen atom from phenol group of Picric acid to amino group of L-Valine is studied. The impact of this occurrence of motion in the molecular structure is also discussed. The vibrational sequence pattern of the weak interaction molecule is analyzed. Moreover, ¹³C NMR and ¹H NMR are calculated by using the gauge independent atomic orbital (GIAO) method with B3LYP methods and the 6-311++G(d,p) basis set and their spectra are simulated and the chemical shifts related to TMS are compared. A study on the electronic and optical properties; absorption wavelengths, excitation energy, dipole moment and frontier molecular orbital energies, are performed by HF and DFT methods. The calculated HOMO and LUMO energies (kubo gap) are displayed in the figures which show that the occurring of charge transformation within the molecule. Besides frontier molecular orbitals (FMO), molecular electrostatic potential (MEP) was performed. NLO properties related to Polarizability and hyperpolarizability is also discussed.

Keywords: L-Valine; optical properties; gauge independent atomic orbital; Chemical shifts; FMO.

1. Introduction

L-Valine is also aliphatic nonpolar chain having both a primary amino group and a carboxyl group in which the proton is exchanged between them. So the amino acid exists as zwitterions [1]. In this respect, the resources with amino acids are interesting materials for NLO applications. The amino acids contain asymmetric carbon atoms which make it optically active and most of them crystallize in non centrosymmetric space groups. Bulk crystals of amino acids have physical properties, which makes them ideal candidates for nonlinear optical devices. The aromatic systems in conjugated with nitro group leading to charge transfer systems, have been intensely studied and their crystals are highly recognized as the materials of the future because their

molecular nature combined with versatility of synthetic chemistry can be used to alter their structure in order to maximize the non-linear properties [2-4].

The nitro substituted phenols with high optical non-linearities are very promising materials for future optoelectronic and non-linear optical applications. The crystals made by the combinations of L-Valine and Picric acid offer excellent non linearities applications in various fields like telecommunication, optical computing, optical data storage and optical information processing. L-valinium picrate is a promising NLO material in which L-valine acts as donor and the picric acid as electron acceptor which provides the ground state charge asymmetry of the molecule required for second-order nonlinearity. In the present investigation a systematic study is carried out on the growth and some of the characterization of L-valinium picrate (LVP). Investigations of amino acid picrates have attracted the attention of researchers in the recent precedent [5-7]. In this work, the FT-IR and FT-Raman experimental investigation and computational calculations (¹³C NMR and ¹H NMR, UV-Visible) Frontier molecular studies have been carried out on L-Valinium Picrate.

2. Experimental details

The L-Valinium Picrate crystal is of spectroscopic grade used for recording the spectra as such without any further purification. The FT-IR spectrum of the compound is recorded in Bruker IFS 66V spectrometer in the range of 4000–400 cm⁻¹. The spectral resolution is ± 2 cm⁻¹. The FT-Raman spectrum of L-Valinium Picrate crystal is also recorded in the same instrument with FRA 106 Raman module equipped with Nd:YAG laser source operating at 1.064 µm line widths with 200 mW power. The spectra are recorded in the range of 4000–100 cm⁻¹ with scanning speed of 30 cm⁻¹ min⁻¹ of spectral width 2 cm⁻¹. The frequencies of all sharp bands are accurate to ± 1 cm⁻¹.

3. Computational methods

In the present work, HF and some of the hybrid methods; LSDA, B3LYP and B3PW91 are carried out using the basis sets 6-311++G(d,p). All these calculations are performed using GAUSSIAN 09W [8] program package on Pentium IV processor in personal computer. In DFT methods; local-spin density approximation LSDA generally predicts a better molecular geometries, vibrational frequencies and charge densities in strongly bounded systems. Becke's three parameter hybrids function combined with the Lee-Yang-Parr correlation function (B3LYP) [9-10], Becke's three parameter exact exchange-function (B3) [11] combined with gradient-corrected correlational functional of Lee, Yang and Parr (LYP) [12-13] and Perdew and Wang (PW91) [14-15] predict the best results for molecular geometry and vibrational frequencies for moderately larger molecules.

The calculated frequencies are scaled down to yield the coherent with the observed frequencies. The scaling factors are 0.903, 0.896 and 1.1 for HF/6-311++G(d,p) method. For LSDA/6-311++G(d,p) basis set, the scaling factors are 0.962, 1.04 and 1.1. For B3LYP/6-311++G(d,p) basis set, the scaling factors are 0.952, 1.056 and 1.03. For B3PW91/6-311++G(d,p) basis set, the scaling factors are 0.912,0.889, 0.952, 1.02 and 0.980, 0.945, 0.970 and 1.02. The optimized molecular structure of the molecule is obtained from Gaussian 09 and Gauss view program and is shown in Figure 1. The comparative optimized structural parameters such as bond length, bond angle and dihedral angle are presented in Table 1. The observed (FT-IR and FT-Raman) and calculated vibrational frequencies and vibrational assignments are submitted in Table 2. Experimental and simulated spectra of IR and Raman are presented in the Figures 2 and 3, respectively.

The ¹H and ¹³C NMR isotropic shielding are calculated with the GIAO method [16] using the optimized parameters obtained from B3LYP/6-311++G(d,p) method. ¹³C isotropic magnetic shielding (IMS) of any X carbon atoms is made according to value ¹³C IMS of TMS, CS_X =IMS_{TMS}-IMS_x. The ¹H and ¹³C isotropic chemical shifts of TMS at B3LYP methods with 6-311++G(d,p) level using the IEFPCM method in DMSO. The absolute chemical shift is found between isotropic peaks and the peaks of TMS[17].

The electronic properties; HOMO-LUMO energies, absorption wavelengths and oscillator strengths are calculated using B3LYP method of the time-dependent DFT (TD-DFT) [18-19], basing on the optimized structure in gas phase and solvent [DMSO and ethanol] mixed phase. Thermodynamic properties of L-Valine at 298.15°C have been calculated in gas phase using B3LYP/6-311++G(d,p) method. Moreover, the dipole moment, nonlinear optical (NLO) properties, linear polarizabilities and first hyperpolarizabilities and chemical hardness have also been studied.

4. Results and discussion

4.1. Molecular geometry

The molecular structure of L-Valinium picrate belongs to C_s point group symmetry. The optimized structure of the molecule is obtained from Gaussian 09 and Gaussview program [12] and is shown in Figure 1. The present molecule contains L-Valine and Picrate. Both are connected by Vander walls interactions. The interactions are created in between OH group of the picrate molecule and amino group of L-Valine. By this interaction, the H atom of phenol group is detached and moved towards amino group and thereby H atom without making the bond weakly coupled with amino group. Thus the NH₂ becomes NH₃ and both the molecules fascinated with each other. The bond lengths of N25-N26 and N25-N28 are 1.015Å and 1.022Å respectively, whereas the Vander walls bond length of N25-N27 is 1.115Å. The value of Vander walls bond length is lies between two N-H bonds in amine group. The entire atoms of L-Valine molecule are situated in multiple planes whereas the Picrate molecule positioned in one plane except slight twisting of one



 NO_2 group. The planes of both the molecules are located perpendicularly due to the attractive forces existed between O and H.

4.2. Vibrational assignments

In order to obtain the spectroscopic signature of the L-Valiniumpicrate compound, the computational calculations are performed for frequency analysis. The molecule, has C_s point group symmetry, consists of 38 atoms, so it has 108 normal vibrational modes. On the basis of Cs symmetry, the 108 fundamental vibrations of the molecule can be distributed as 63 in-plane vibrations of A' species and 45 out of plane vibrations of A'' species, i.e., $\Gamma_{vib} = 63 \text{ A'} + 45 \text{ A''}$. In the C_s group symmetry of molecule is non-planar structure and has the 108 vibrational modes span in the irreducible representations.

The harmonic vibrational frequencies (unscaled and scaled) calculated at HF, B3LYP and B3PW91 levels using the triple split valence basis set along with the diffuse and polarization functions, 6-311++G(d,p) and observed FT-IR and FT-Raman frequencies for various modes of vibrations have been presented in Tables 2 and 3. Comparison of frequencies calculated at HF and LSDA/B3LYP/B3PW91 with the experimental values reveal the over estimation of the calculated vibrational modes due to the neglect of a harmonicity in real system. Inclusion of electron correlation in the density functional theory to certain extends makes the frequency values smaller in comparison with the HF frequency data. Reduction in the computed harmonic vibrations, although basis set sensitive is only marginal as observed in the DFT values using 6-311+G(d,p).

4.2.1. Amino group vibrations

The O-H bond in phenol of picrate is broken down and the hydrogen is attracted by the N of the amino group and Vander walls attraction existed between N-H to form NH₃ in L-Valine. Because of the removal hydrogen from O-H group, the double bond is created between C and O forms C=O. Aliphatic primary amines salts are characterized by strong absorption in the region of 3200-2800 cm⁻¹ due to the asymmetric and symmetric NH₂⁺ stretching[20-22]. Free amino acids also have – NH₃ stretching and deformation vibrations. In the solid phase, a broad absorption of medium intensity is observed in the region 3200-3000 cm⁻¹due to the asymmetric –NH₃⁺ stretching vibration. Weak bands due to the symmetric stretching of the –NH₃⁺ group are observed near 2600 cm⁻¹ and 2100 cm⁻¹. A fairly strong –NH₃⁺ deformation band is observed at 1550-1485 cm⁻¹ and a weaker band, which is not resolved for most amino acids, at 1660-1590 cm⁻¹[23-24]. In this present case, the N-H stretching frequencies are observed at 3300, 3270 and 2840 cm⁻¹. The first and second bands are assigned to asymmetric and third are assigned to symmetric vibration. The first two bands are within the expected region whereas the third band suppressed much since the band is from Vander walls bond. The NH₃ symmetric deformation is observed at 1440cm⁻¹ as a very strong peak. This peak is shifted down to the lower region due to the H is attracted by O. The

 NH_2^+ asymmetric and in plane bending wave numbers are found at 1395 and 1375 cm⁻¹. The out of plane bending vibrations are normally identified in the region 1150–900 cm⁻¹ [25-26]. The out of plane bending vibrations are set up with medium and strong intensity at 940 and 930 cm⁻¹. The N-H in plane bending vibrations are moved down while out of plane bending vibrations are observed within the region. This view is clearly shows that the in plane bending are disturbed by other nearby vibrations. The NH₂ twisting signal is raised at the last part of the spectrum.

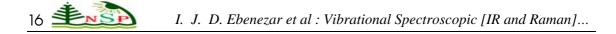
4.2.2. COOH group vibrations

Free amino acids also have carboxilate ion $(CO_2^{-1} \text{ ion})$ stretching vibrations, a strong band occurring in the region 1600-1560 cm⁻¹. Dicarboxylic acids have a strong band due to C=O stretching vibration of the carboxyl group at 1755-1700 cm⁻¹ and another strong band at 1230-1215 cm⁻¹ due to the stretching of the C-O bond[27-28]. According to the literature, two strong bands are identified at 1725 and 1720 cm⁻¹ for C=O stretching vibrations. The C=O band is elevated up to the top of the expected region due to the favoring of hydrogen bond. A strong signal for C-O is observed at 1325 cm⁻¹ and the corresponding in and out of plane bending vibrations are found at 550 and 320 cm⁻¹ respectively. These vibrations have not been affected by other vibrations in the molecule.

The amino acid has hydroxyl stretching vibrations are generally [29] observed in the region around 3500 cm⁻¹. The O-H group vibrations are likely to be the most sensitive to the environment, so they show pronounced shifts in the spectra of the hydrogen bonded species. The band due to the O-H stretching is of medium to strong intensity in the infrared spectrum, although it may be broad. The strong band appeared at 3550 cm^{-1} in the IR spectra is assigned to O–H stretching mode of vibration. The O-H in-plane bending vibration is observed in the region 1440–1260 cm⁻¹ [30]. The O-H out-of-plane deformation vibration for phenol put down in the region 290-320 cm⁻¹ for free O-H and in the region 517-710 cm⁻¹ for associated O-H [25]. In both inter-molecular and intramolecular associations, the wavenumber is at higher value than that in the free O-H. The wavenumber increases with hydrogen bond strength because of large amount of energy required to twist the O-H bond [31]. The calculated values of in-plane and out-of-plane bending vibrations of hydroxyl group are 1370 and 795cm⁻¹, respectively. The carbonyl group is most important in the infrared spectrum because of its strong intensity of absorption and high sensitivity toward relatively minor changes in its environment. Intra- and intermolecular factors affect the carbonyl absorptions in common organic compounds due to inductive, mesomeric effects, field effects and conjugation effects. The entire bending vibrations have much influenced and moved up to the higher region.

4.2.3. C-H Vibrations

For simplicity, modes of vibrations of aromatic compounds are considered as separate ring C-H or C-C vibrations. However, as with any complex molecules, vibrational interactions



occur and these labels only indicate the predominant vibration. Substituted benzenes have large number of sensitive bands, that is, bands whose position is significantly affected by the mass and electronic properties, mesomeric or inductive, of the substituents. According to the literature [32-33] in infrared spectra, most mono nuclear and poly nuclear aromatic compounds have three or four peaks in the region 3000 – 3100 cm⁻¹ [34], these are due to the stretching vibrations of the ring C-H bonds. Accordingly, in the present study, three C-H stretching vibrations are observed at 2980 and 2970 cm⁻¹. These assigned frequencies are shifted down to the observed region which is strongly indicates that the ring vibrations affected much by the substitutions. The C-H in-plane and out-of-plane bending vibrations generally lies in the range 1000 - 1300cm⁻¹ and 950 - 800 cm⁻¹ [35-37] respectively. Three C-H in-plane bending vibrations are observed at 940 and 935 cm⁻¹. According to the literature, the in-plane and out-of-plane bending vibrations are observed at 940 and 935 cm⁻¹.

4.2.4. Methyl group vibrations

The side chain of L-Valine has two methyl groups attached to the C atom. The CH₃ stretching and deformation vibrations are more or less localized, and offer to good group frequencies. The positions of the C-H stretching vibrations are among the most stable in the spectrum. Since the CH₃ group also exhibit C_s symmetry. In aliphatic compounds, the asymmetric and symmetric CH₃ stretching vibrations are normally observed in the region 2950- 2850 cm⁻¹[38-40]. In the present compound, the C-H stretching vibrations are found at 2950, 2930, 2920, 2910, 2890 and 2880 cm⁻¹. The entire vibrational bands are situated in the middle part of the C-H vibrational region of the spectra. The first four of the above are asymmetric and rest of others are symmetric vibrations. The C-H in plane and out of plane bending vibrations are found normally in the region of 1250-1000 cm⁻¹ and 970-700 cm⁻¹ respectively[41-42]. Accordingly, the in plane bending group frequencies are identified at 920, 900, 870, 850, 835 and 830cm⁻¹. All the bending vibrations are observed within the expected region. This view shows that, there is no influence of other vibrational sign on the methyl group vibrations.

Predicted by the DFT calculations, in aliphatic compounds containing CH₃ group, the series of the bands appearing as asymmetric and symmetric deformation modes in the region 1400-1500 cm⁻¹ [43-45] are mainly due to methyl deformation, coupling with the C-H and C-C stretching frequencies, two different extends and in different way. In the present study, the Raman bands at 1440 cm⁻¹ (very strong) and 1420 cm⁻¹ (strong) are attributed to the asymmetric deformation modes of isopropyl group. Appearance of these bands is due to presence of two independent CH₃ groups in the amino acid residues in different environments. The symmetric deformation mode of

isopropyl group normally exhibits relatively two very strong bands at 1440 and 1420 cm⁻¹. They are due to the interaction between hydrogen atoms in two different methyl groups depending upon whether they are moving either closer or away from each other's way [45]. The methyl twisting vibrational signals highlighted at 140 and 120cm⁻¹ in Raman spectrum.

4.2.5. C-CH₃ Vibrations

The title molecule contains two methyl groups in molecular chain, there are two C-CH₃ stretching vibrations are possible. The C-CH₃ vibrations usually combine with C-H in-plane bending vibration [46]. According to which, the active fundamentals are appeared with medium intensity at 1105 and 1090 cm⁻¹ in IR and Raman are identified as C-CH₃ stretching vibration. The C-CH₃ in-plane bending vibration is found at 280 and 260cm⁻¹ and out-of-plane bending vibration is found at 190 and 150cm⁻¹. As reported in the literature [47-48], all the above C-CH₃ vibrations deviated much from the expected range. This is purely due to the repulsion between methyl groups.

4.2.6. CC Vibrations

Generally, the C=C stretching vibrations in aromatic compounds are seen in the region of 1430-1650 cm⁻¹ [49-51]. The C=C stretching vibrations of title compound are observed with very strong intensity at 1670, 1650 and 1640 cm⁻¹. The stretching vibrational bands for C-C bond are observed at 1550, 1540 and 1490 cm⁻¹. All bands lie in the top end of the expected range when compared to the literature values. The CCC in-plane bending vibrations are observed at 700, 660 and 650 cm⁻¹ and the out-of-plane bending vibrations are appeared at 450, 420 and 400 cm⁻¹. These assignments are in good agreement with the literature [52-53]. The C-C vibrations in the L-Valine are found at 1310, 1085 and the in plane and out of plane bending vibrations are identified at 720 and 710 cm⁻¹ and 250 and 220 cm⁻¹. The CC vibrational signals are observed within the expected region. But the bending vibrations are in out of the region due to the attraction of nearby vibrations.

4.2.7. Nitro group vibrations

Aromatic nitro compounds have strong absorptions due to asymmetric and symmetric stretching vibrations of the NO₂ group at 1570-1485 and 1370-1320 cm⁻¹, respectively, Hydrogen bonding has a little effect on the NO₂ asymmetric stretching vibrations [54-55]. In the present case, very strong bands at 1620, 1600 and 1590 cm⁻¹ and 1485, 1475 and 1450 cm⁻¹ have been assigned to asymmetric and symmetric stretching modes of NO₂. Each one of both the stretching vibrations are moved up drastically from the expected region. This realignment of the vibrations is purely due to the inductive effect of H of Phenol. Aromatic nitro compounds have a band of weak to medium intensity in the region 590 – 500 cm⁻¹[56] due to the out of plane bending deformations mode of NO₂ group. This is observed with strong intensity at 530, 510 and 500 cm⁻¹ for the title compound.

The in plane NO₂ deformation vibrations have a week to medium absorption in the region 775-660 cm-1 [57-58]. In the present case, the NO₂ deformation is found at 780, 740 and 730 cm⁻¹. The NO₂ twisting vibrations are observed at 60, 50 and 40 cm⁻¹. One band of in plane bending pushed up and entire bands of out of plane bending are within the region which is mainly due to OH.

4.2.8. C-N vibrations

18

The C-N stretching signal is raised in the region of 1350-1000 cm⁻¹ [59]. In the present compound, the C-N stretching vibrations are observed at 1370, 1350 and 1340 cm⁻¹. The C-N bending vibrations of a nitro group take place around 870 and 610 cm⁻¹, respectively [60]. The C-N in-plane bending of a nitro group for the title compound assigned at 630, 610 and 560 cm⁻¹, respectively. The C-N out-of-plane bending vibrations are found at 390, 360 and 340 cm⁻¹. Some of the assigned values of C-N stretching and bending vibrations are observed at out of the expected region. The repulsion between the NO₂ reduce the wavenumber of normal mode of vibrations.

4.2.9. CCN vibrations

In amino acids, the absorption bands corresponding to C-C-N stretching vibrations are observed in the wave number region $1150-850 \text{ cm}^{-1}$ [61-62]. In the title molecule, a strong IR and weak Raman band at 1270 cm⁻¹ is attributed to the C-C-N symmetric stretching vibration. However the much-expected strong IR counterpart is not found distinctly as it overlaps with the degenerate stretching mode of the anion due to lifting of degeneracy. The strong peak at 1105 cm⁻¹ is due to C-N antisymmetric stretching vibration. The wave numbers at 1050 and 900 cm⁻¹ are attributed to C-C stretching vibrations. The in-phase and out-of-phase vibrations of skeletal carbon have also been identified 530 and 320 cm⁻¹. These vibrations are degenerated with other bending vibrations.

4.3. NMR analysis

NMR spectroscopy is currently used for structure elucidation of complex molecules. The combined use of experimental and computational tools offers a powerful gadget to interpret and predict the structure of bulky molecules. The optimized structure of L-Valinium Picrate is used to calculate the NMR spectra at B3LYP method with 6-311++G(d,p) level using the GIAO method and the chemical shifts of the compound are reported in ppm relative to TMS for ¹H and ¹³C NMR spectra which are presented in Tables 4. The corresponding spectra are shown in Figure 8.

In view of the range of ¹³C NMR chemical shifts for organic molecules usually is >100 ppm [64-65] the accuracy ensures reliable interpretation of spectroscopic parameters. In the present work, ¹³C NMR chemical shifts of some carbons in the ring and chain are >100 ppm, as in the in the Table 4.

In the case of picrate, the chemical shift of C1, C3, C7, C9, C13 and C15 are 76.09, 91.9, 115.3, 114.9, 68.2 and 70.0 ppm respectively. The shift is more in C7 than rest of others. This is mainly for the formation of double bridge between C7 and O8 due to the broken of paramagnetic proton shield by the substitution of C instead of COOH. The N10 in the chain has more shifted (167ppm) due to the addition of one more hydrogen atom which is migrated from OH group. The shift of the entire carbons of the ring is found increased slightly when going from gas to solvent due to the solvent effect. The chemical shift values of oxygen have not changed due to the solvent effect. The chemical shift is greater in C22 than C31 and C35 due to the loading difference between COOH and CH₃. The H28 atom is more shifted than H26 and H27 due to the zwitter ion effect.

The effect of migration of H atom from OH to NH_2 produces the change of physical (NLO), chemical (semiconductor) and electronic (decrement of energy gap) properties of the L-Valine Picrate from L-Valine and Picrate. There is no change of chemical shift in N and O due to the rigidity of the diamagnetic shielding of the atom. From the molecular geometry, it is observed that, there is lot of change of geometries of molecule due to the existence of attractive force between L-Valine and Picrate. This view is also evident that the enhancement of the NLO property of the present molecule.

4.4. Electronic properties (frontier molecular analysis)

The frontier molecular orbitals are very much useful for studying the electric and optical properties of the organic molecules and directly explore the occurring of inter-charge transformation in the molecule. The stabilization of the bonding molecular orbital and destabilization of the antibonding can increase when the overlap of two orbitals increases. In the molecular interaction, there are the two important orbitals that interact with each other. One is the highest energy occupied molecular orbital is called HOMO represents the ability to donate an electron. The other one is the lowest energy unoccupied molecular orbital is called LUMO as an electron acceptor. These orbitals are sometimes called the *frontier* orbitals. The interaction between them is much stable and is called filled empty interaction.

The 3D plots of the frontier orbitals, HOMO and LUMO for L-Valinium Picrate molecule are in gas, shown in Figures 4 and 6. According to Figures 4, the HOMO is mainly localized over the ring CCC, NO₂ of Picrate and methyl group of L-Valine chain. The entire C in the chain is connected by SP³ orbital lobes. The SP³ orbital lobe of C overlapped with SP³ of NO₂ and nearby =CO group. However, LUMO is characterized by a charge distribution connects the part of ring of



CCC, NO₂. When two same sign orbitals overlap to form a molecular orbital, the electron density will occupy at the region between two nuclei. The molecular orbital resulting from in-phase interaction is defined as the bonding orbital which has lower energy than the original atomic orbital. The out of phase interaction forms the anti bonding molecular orbital with the higher energy than the initial atomic orbital. From this observation it is clear that the in and out of phase interaction are present in HOMO and LUMO respectively. The HOMO \rightarrow LUMO transition implies an electron density transferred among CCC, NO₂ of Picrate and CH₃, NH₃ and COO groups. The HOMO and LUMO energy are 7.1223 eV and 4.8003 eV in gas phase (figure 4). Energy difference between HOMO and LUMO orbital is called as energy gap (kubo gap) that is an important for electrical conductivity and stability of structures. The DFT level calculated energy gap is 2.322 eV, show the lower energy gap and reflect the very effective electrical activity of the molecule. From the energy gap is also inferred that, the L-Valinium Picrate has semiconductor property. The energy gap of L-Valine and Picrate molecules are 7.0981 eV and 4.355eV respectively whereas when both the compounds combined to form L-Valinium Picrate, the energy gap(2.322 eV) is considerably decreased and expose its enormous electrical property.

4.5. Optical properties (HOMO-LUMO analysis)

The UV and visible spectroscopy is used to detect the presence of chromophores in the molecule and whether the compound has NLO properties or not. The calculations of the electronic structure of L-Valinium Picrate are optimized in singlet state. The low energy electronic excited states of the molecule are calculated at the B3LYP/6-311++G(d,p) level using the TD-DFT approach on the previously optimized ground-state geometry of the molecule. The calculations are performed for title molecule in gas phase and with the solvent of ethanol and DMSO. The calculated excitation energies, oscillator strength (*f*) and wavelength (λ) and spectral assignments are given in Table 7. The major contributions of the transitions are designated with the aid of SWizard program [63].

TD-DFT calculations predict three transitions in the visible region. In the case of gas phase, the strong transition is at 593.71, 498.32 and 488.33 nm with an oscillator strength f=0.001, 0.005 and 0.0007 with 2.2, 2.4 and 2.5 eV energy gap. The transition is $n\rightarrow\pi^*$ in visible region. The designation of the band is R-band (German, radikalartig) which is attributed to above said transition of single chromophoric groups, such as C=O group. They are characterizes by low molar absorptivities (ξ_{max} <100) and undergo hypsochromic shift with an increase in solvent polarity. The simulated UV-Visible spectra in gas and solvent phase of L-Valinium Picrate are shown in figure 7.

In the case of DMSO solvent, strong transitions are 497.68, 406.78 and 393.82 nm with an oscillator strength f=0.00, 0.003 and 0.003 with minimum energy gap 2.49, 314 and 3.14 eV. They are assigned to $n \rightarrow \pi^*$ transitions and belongs to visible region. This view shows that, since all the transitions are positioned at visible region, the L-Valinium Picrate molecule colored and it is

capable of having rich NLO properties than L-Valine and Picrate separately. In addition to that, the calculated optical band gap 2.419 eV which ensure that the present compound is optically very active. In view of calculated absorption spectra, the maximum absorption wavelength corresponds to the electronic transition from the HOMO to LUMO with maximum contribution. In this present compound, the chromophores is CH_3 group, the properties are changed and enhanced from L-Valine + Picrate to L-Valinium Picrate.

The chemical hardness and potential, electronegativity and Electrophilicity index are calculated and their values are shown in Table 5. The chemical hardness is a good indicator of the chemical stability. The chemical hardness is increased slightly (1.43-2.07) in going from Gas to solvent (DMSO). Hence, the present compound has much chemical stability. Similarly, the electronegativity is increased from 3.85 up to 4.10, from gas to solvent, if the value is greater than 1.7; the property of bond would be changed from covalent to ionic. Accordingly, the bonds in the compound converted from covalent to ionic and are independent of solvent. Electrophilicity index is a measure of energy lowering due to maximal electron flow between donor [HOMO] and acceptor [LUMO]. From the table 5, it is found that the Electrophilicity index of L-Valinium Picrate is 5.171 in gas and 8.099 in solvent, which is very high and this value ensure that the strong energy transformation between HOMO and LUMO. The dipole moment in a molecule is another important electronic property. Whenever the molecule has larger the dipole moment, the intermolecular interactions are very strong. The calculated dipole moment value for the title compound is 23.13 Debye in gas and 27.10 in solvent. It is too high which shows that; the L-Valinium Picrate molecule has strong intermolecular interactions.

4.6. Molecular electrostatic potential (MEP) maps

The molecular electrical potential surfaces illustrate the charge distributions of molecules three dimensionally. This map allows us to visualize variably charged regions of a molecule. Knowledge of the charge distributions can be used to determine how molecules interact with one another and it is also be used to determine the nature of the chemical bond. Molecular electrostatic potential is calculated at the B3LYP/6-311++G(d,p) optimized geometry. There is a great deal of intermediary potential energy, the non red or blue regions indicate that the electro negativity difference is not very great. In a molecule with a great electro negativity difference, charge is very polarized, and there are significant differences in electron density in different regions of the molecule. This great electro negativity difference leads to regions that are almost entirely red and almost entirely blue. Greater regions of intermediary potential, yellow and green, and smaller or no regions of extreme potential, red and blue, are key indicators of a smaller electronegativity.

The color code of these maps is in the range between -8.25 a.u. (deepest red) to 8.25 a.u. (deepest blue) in compound. The positive (blue) regions of MEP are related to electrophilic

reactivity and the negative (green) regions to nucleophilic reactivity shown in Figure 5. As can be seen from the MEP map of the title molecule, the negative regions are mainly localized over the NO_2 group of Picrate molecule. A maximum positive region is localized on the amine and methyl groups of L-Valine molecule indicating a possible site for nucleophilic attack. The MEP map shows that the negative potential sites are on electronegative atoms (O atom) as well as the positive potential sites are around the amine and methyl groups. From these results, it is clear that the methyl groups indicate the strongest attraction and NO_2 group indicates the strongest repulsion.

4.7. Polarizability and First order hyperpolarizability calculations

In order to investigate the relationships among molecular structures and non-linear optic properties (NLO), the polarizabilities and first order hyperpolarizabilities of the L-Valinium Picrate compound was calculated using DFT-B3LYP method and 6-311+G(d,p) basis set, based on the finite-field approach.

It is well known that, molecule with high values of dipole moment, molecular polarizability, and first hyperpolarizability having more active NLO properties. The first hyperpolarizability (β) and the component of hyperpolarizability β_x , β_y and β_z of L-Valine along with related properties (μ_0 , α_{total} , and $\Delta \alpha$) are reported in Table 7. The calculated value of dipole moment is found to be 7.465 Debye. The highest value of dipole moment is observed for component μ_X . In this direction, this value is equal to 7.081 D. The lowest value of the dipole moment of the molecule compound is μ_Z component (-0.281D). The calculated average polarizability and anisotropy of the polarizability is 258.82x10⁻²⁴ esu and 548.29x10⁻²⁴ esu, respectively. The magnitude of the molecular hyperpolarizability β , is one of important key factors in a NLO system. The B3LYP/6-311+G(d,p) calculated first hyperpolarizability value (β) is 217.85x10⁻³⁰ esu. From the above results, it is observed that, the molecular Polarizability and hyperpolarizability of the title compound in all coordinates are active. So that, the L-Valinium Picrate can be used to prepare NLO crystals and those crystal is able to produce second order second harmonic waves with more amplitude.

5. Conclusion

In the present investigation, a detailed vibrational and electronic spectral analysis has been carried out for the L-Valine Picrate. The optimized geometries, bond length, bond angle, dihedral angle, kubo gap Polarizability and hyperpolarizability are determined and analyzed theoretically by

ab initio-HF and DFT (LSDA, B3LYP and B3PW91) methods with 6-31G (d, p) and 6-311G (d, p) basis sets. From the analysis, the following observations are made.

- 1. On the basis of Cs symmetry, there are 108 fundamental vibrations of the molecule are observed with sufficient peak intensity. Of the 108 vibrations 63 in-plane vibrations and 45 out of plane vibrations.
- 2. The first two bands of N-H stretching are within the expected region whereas the third band suppressed much since the band is from Vander walls bond.
- 3. The entire O-H bending vibrations have much influenced and moved up to the higher region.
- 4. All the CH₃ bending vibrations are observed within the expected region. This view shows that, there is no influence of other vibrational sign on the methyl group vibrations.
- 5. Each one of both the N-O stretching vibrations are moved up drastically from the expected region. This realignment of the vibrations is purely due to the inductive effect of H of Phenol.
- 6. From the HOMO and LUMO observation, it is clear that the in and out of phase interaction are present in HOMO and LUMO respectively. The HOMO→LUMO transition implies an electron density transferred among CCC, NO₂ of Picrate and CH₃, NH₃ and COO groups.
- 7. The DFT level calculated energy gap is 2.322 eV, show the lower energy gap and reflect the very effective electrical activity of the molecule. From the energy gap is also inferred that, the L-Valinium Picrate has semiconductor property.
- 8. The energy gap of L-Valine and Picrate molecules are 7.0981 eV and 4.355eV respectively whereas when both the compounds combined to form L-Valinium Picrate, the energy gap(2.322 eV) is considerably decreased and expose its enormous electrical property.
- 9. From the MEP results, it is clear that the methyl groups indicate the strongest attraction and NO₂ group indicates the strongest repulsion.
- 10. From the Polarizability and hyperpolarizability results, it is observed that, the molecular Polarizability and hyperpolarizability of the title compound in all coordinates are active. So the L-Valinium Picrate can be used to prepare NLO crystals and those crystals are able to produce second order second harmonic waves with more amplitude.

References

- [1] S. Moitra and T. Kar, Cryst. Res. Technol., 45, 70-74 (2010).
- [2] N. Vijayan, R. Ramesh Babu, R. Gopalakrishnan, P. Ramasamy, W.T.A. Harrison, J. Cryst. Growth 262, 490–498 (2004).
- [3] Y. Goto, A. Hyashi, Y. Kimura, S.M. Nakayama, J. Cryst. Growth, 108, 688–698 (1991).
- [4] M. Arivazhagan, S. Jeyavijayan, Spectrochimica Acta Part A, 79, 376–383 (2011).

- [5] P. Srinivasan, T. Kanagasekaran, R. Gopalakrishnan, G. Bhagavannarayana, P. Ramasamy, Cryst. Growth Des., 6, 1663 (2006).
- [6] Martins, T. S., Matos, J. R., Vicentini, G., Isolani, P. C., J. Therm. Anal. Calorimetry, 86, 351 (2006).
- [7] Devi, T. U., Lawrence, N., Babu, R. R., Ramamurthi, K., J. Cryst. Growth, 310, 116 (2008).
- [8] R.J. Lewis, Sr (Ed.). Hawley's Condensed Chemical Dictionary, 12th ed. New York, NY: Van Nostrand Rheinhold Co., 860 (1993).
- [9] D. Hartley and H. Kidd (eds.). The Agrochemicals Handbook. Old Woking, Surrey, United Kingdom: Royal Society of Chemistry/Unwin Brothers Ltd., (1983).
- [10] W. Gerhartz, Ullmann's Encyclopedia of Industrial Chemistry. 5th ed: Deerfield Beach, FL: VCH Publishers, 21, (1985).
- [11] M.K. Marchewka, A. Pietraszko, Spectrochimica Acta Part A, 69, 312-318 (2008).
- [12] Ivan S. Lim, Gustavo E. Scuseria, Chemical Physics Letters, 460, 137-140 (2008).
- [13] Ljupco Pejov, Mirjana Ristova, Bojan Soptrajanov, Spectrochimica Acta Part A, 79, 27-34 (2011).
- [14] M.J. Frisch et al., Gaussian 09, Revision A.1, Gaussian, Inc., Wallingford CT, (2009).
- [15] Z. Zhengyu, D. Dongmei, Journal of Molecular Structure (Theochem), 505, 247-252 (2000).
- [16] Z. Zhengyu, F. Aiping, D. Dongmei, Journal of Quantum Chemistry, 78, 186-189 (2000).
- [17] A.D. Becke, Physics Review, A 38, 3098-3101 (1988).
- [18] C. Lee, W. Yang, R.G. Parr, Physics Review, B., 37, 785-790, (1988).
- [19] A.D. Becke, Journal of Chemical Physics, **98**, 5648-5652 (1993).
- [20] R.M. Silverstein, F.X. Webster, Spectrometric Identification of Organic Compounds, sixth ed., Wiley, New York, (1998).
- [21] S. Pandiarajan, M. Umadevi, R.K. Rajaram, V. Ramakrishnan, Spectrochimica Acta Part A, 62, 630-636 (2005).
- [22] J.R. During, M.M. Bergana, H.V. Phan, Journal of Raman Spectroscopy, 22, 141 (1991).
- [23] M. Tsuboi et al., Spectrochimica, Acta, , **19**, 271-275 (1963).
- [24] E. Steger et al., Spectrochimica, Acta, , 19, 293-297 (1963).
- [25] G. Varsanyi, Vibrational spectra of benzene derivatives, Academic press, New York, (1969).
- [26] N. Vijayan, R.R. Babu, R. Gopalakrishnan, P. Ramasamy, M. Ichimura, M. Palanichamy, Journal of Crystal Growth, 564–569 (2005).
- [27] G.B.B.M. Sutherland, Advanced Protein chemistry, 7, 291 (1952).
- [28] R.J. Koegel et al., Journal American chemical society, 77, 5708 (1955).
- [29] D. Michalska, D.C. Bienko, A.J.A. Bienko, Z. Latajaka, J. Phys. Chem., 100, 17786–17790 (1996).
- [30] D.N. Sathyanarayana, Vibrational Spectroscopy—Theory and Applications, second ed., New Age International (P) Limited Publishers, New Delhi, (2004).
- [31] I.D. Sadekov, Russian Chemical Review, 30, 179–195 (1970).
- [32] George Socrates, Infrared and Raman Characteristic group frequencies, 3rd edition, Wiley, New York. (2001).
- [33] G. Eazhilarasi, R. Nagalakshmi, V. Krishnakumar, Spectrochimica Acta part A, 71, 502 507 (2008).
- [34] G. Varsanyi, Assignments of Vibrational Spectra of Seven Hundred Benzene Derivatives, 1–2, Adam Hilger, (1974).
- [35] V. Krishnakumar, N. Prabavathi, Spectrochimica Acta part A, 71, 449-457 (2008).
- [36] A. Altun, K. Golcuk, M. Kumru, Journal of Molecular structure (Theochem.), 637, 155 (2003).
- [37] S.J. Singh, S.M. Pandey, Indian Journal of Pure and applied physics, 12, 300-305 (1974).
- [38] G. Socrates, Infrared and Raman Characteristics Group Frequencies, Wiley, New York, (2000).
- [39] M. Silverstein, G. Clayton Basseler, C. Morrill, Spectrometric identification of organic Compounds, John Wiley, New York, (1991).
- [40] C. Brian Smith, Infrared Spectral Interpretation, CRC Press, New York, (1999).
- [41] A. Altun, K. Go ' Icu'k, M. Kumru, Journal of Molecular structure (Theochem), 625, 17-20 (2003).
- [42] J.R. Durig, M.M. Bergana, H.V. Phan, Journal of Raman spectroscopy, 22, 141-146 (1991).
- [43] J.H.S. Green, D.J. Harrison, W. Kynoston, Spectrochimica Acta, 27A, 807-810 (1971).
- [44] K. Bahgat, N. Jasem, Talaat El-Emary, Journal of Serbian Chemical Society, 74, 555-571 (2009).
- [45] N.B. Clothup, L.H. Daly and S.E. Wiberley, Introduction to Infrared and Raman spectroscopy, Academic press Inc., London, (1964).
- [46] H.F. Hameka and J.O. Jensen, Journal of Molecular Structure (Theochem), 362, 325-328 (1996).
- [47] R.M. Silverstein, G. Clayton Bassler, T.C. Morrill, Spectrometric Identification of Organic Compounds, John Wiley, New York, (1991).
- [48] D.N. Singh, I.D. Singh, R.A. Yadav, Indian Journal of Physics, 76B, 307 (2002).
- [49] V. Krishna kumar R. John Xavier, Indian Journal of Pure and Applied Physics, 41, 95-99 (2003).



- [50] D.N. Sathyanarayana, vibrational spectroscopy theory and applications, 2nd edition, New AgeInternational (P) limited publisher, New Delhi, (2004).
- [51] P.S. Kalsi, Spectroscopy of Organic Compounds, Wiley Eastern Limited, New Delhi, 117-118 (1993).
- [52] R.L. Peesole, L.D. Shield, I.C. Mcwillam, modern methods of chemical analysis, wiley, New York, (1976).
- [53] A.R. Prabakaran, S. Mohan, Indian Journal of Physics, 63B, 468-473 (1989).
- [54] N.Sundaraganesan, S.Ilakiamani, H.Saleem, P.M. Wojieehowski, D. Michalska, Spectrochimica Acta Part A, 61, 2995 (2005).
- [55] D.N. Sathyanarayana, vibrational spectroscopy theory and application, 2nd edition, New Age International (P) Limited publishers, New Delhi, (2004).
- [56] S.George, Infrared and Raman characteristics group frequencies Tables and charts, 3rd edition, wiley, chichester, (2001).
- [57] V. Krishnakumar, V. Balachandran, Spectrochimica Acta part A, 61, 1811-1819 (2005).
- [58] R. A. Kanna Rao, N. Syam Sunder, Spectrochimica Acta, 49, 1691 (1993).
- [59] M. Silverstein, G.C. Basseler, C. Morill, Spectrometric Identification of Organic Compounds, Wiley, New York, (1981).
- [60] Jag Mohan, Organic Spectroscopy Principles and Applications, Narosa Publishing House, New Delhi, (2000).
- [61] N.B. Colthup, L.H. Daly, S.E. Wiberley, Introduction to Infrared and Raman Spectroscopy, Academic Press, New York, (1990).
- [62] M. Tsuboi, T. Onishi, I. Nakagawa, T. Shimanouchi, S. Mizushima, Spectrochimica Acta, 12, 253 (1958).
- [63] S.I. Gorelsky, SWizard Program Revision 4.5, University of Ottawa, Ottawa, Canada. Available from: http://www.sg.chem.net/, (2010).
- [64] J.H. Vander Maas and E.T.G. Lutz, Spectrochimica Acta, 30A, 2005 (1974).
- [65] S. Ahmad, S. Mathew, P.K. Verma, Indian Journal of Pure and Applied Physics, 30, 764-770 (1992).